

Vascular niche E-selectin regulates hematopoietic stem cell dormancy, self renewal and chemoresistance

Ingrid G Winkler¹, Valérie Barbier¹, Bianca Nowlan², Rebecca N Jacobsen^{2,3}, Catherine E Forristal², John T Patton⁴, John L Magnani⁴ & Jean-Pierre Lévesque^{2,3}

The microenvironment, or niche, surrounding a stem cell largely governs its cellular fate. Two anatomical niches for hematopoietic stem cells (HSCs) have been reported in the bone marrow, but a distinct function for each of these niches remains unclear. Here we report a new role for the adhesion molecule E-selectin expressed exclusively by bone marrow endothelial cells in the vascular HSC niche. HSC quiescence was enhanced and self-renewal potential was increased in E-selectin knockout (*Sele*^{-/-}) mice or after administration of an E-selectin antagonist, demonstrating that E-selectin promotes HSC proliferation and is a crucial component of the vascular niche. These effects are not mediated by canonical E-selectin ligands. Deletion or blockade of E-selectin enhances HSC survival threefold to sixfold after treatment of mice with chemotherapeutic agents or irradiation and accelerates blood neutrophil recovery. As bone marrow suppression is a severe side effect of high-dose chemotherapy, transient blockade of E-selectin is potentially a promising treatment for the protection of HSCs during chemotherapy or irradiation.

HSCs reside in the bone marrow and generate the cells needed to replenish the blood and immune system. This process requires tight regulation, with instructions provided by cues within specific local microenvironments (niches). At least two anatomical HSC niches have been described in the bone marrow: an endosteal or osteoblastic niche within 2–3 cell diameters from the bone–bone marrow interface^{1–5} and an endothelial or (peri-)vascular niche adjacent to bone marrow endothelial sinuses^{6–9}. Whether these two anatomically defined niches have separate functions, and the degree to which factors at these niches control HSC behavior, is under intense investigation¹⁰. The identification of functional components unique to each of these niches would greatly contribute to these investigations.

Endothelial selectins are cell adhesion molecules that are expressed at the vascular HSC niche to which hematopoietic stem and progenitor cells (HSPCs) adhere. The selectins are a family of three cell adhesion molecules with well-characterized roles in leukocyte homing. E-selectin (endothelial selectin) and P-selectin (platelet selectin) are typically expressed by endothelial cells at sites of injury or inflammation, enabling leukocytes with counter-receptors to roll on the activated vasculature¹¹. Consistent with this function, leukocytes in mice deficient for both E- and P-selectin (or their functional receptors) have severely impaired leukocyte migration^{12,13}. However P- and E-selectin are constitutively expressed on bone marrow endothelium^{14–16}, aiding the homing and engraftment of circulating HSPCs^{17,18}. Here we demonstrate an additional role for E-selectin in steady-state hematopoiesis. We show that E-selectin on the bone marrow vasculature directly induces HSC proliferation and chemosensitivity at the expense of HSC self renewal.

RESULTS

HSCs cycle slower when E-selectin is absent in mice

To determine whether the absence of endothelial selectins alters HSC quiescence, we first measured HSC turnover in wild-type (WT) and E-selectin knockout (*Sele*^{-/-}) mice by BrdU incorporation *in vivo*. BrdU is a thymidine analog that is incorporated into genomic DNA during the S phase of cell division. After BrdU administration, we harvested bone marrow cells from the mice and measured the percentage of phenotypic Lin⁻Kit⁺Sca1⁺(LKS⁺)CD34⁻HSCs¹⁹ that had incorporated BrdU. The percentage of HSCs incorporating BrdU steadily increased over time, with 50% of the HSCs in WT mice incorporating BrdU and entering S phase by 3.3 d *in vivo* (Fig. 1a–c). HSC turnover was markedly reduced in *Sele*^{-/-} mice and in mice with knockout alleles of both P- and E-selectin (*Selp*^{-/-}*Sele*^{-/-}); these mice required ~9.5 d for 50% of their HSCs to be BrdU⁺ (2.8-fold slower than WT) (Fig. 1a–c). Notably, this reduced HSC turnover was specific to E-selectin knockout mice, as HSC cycling in P-selectin knockout (*Selp*^{-/-}) mice was similar to that in WT mice (Fig. 1c). We also observed these differences in HSC turnover using other phenotypic markers of HSCs (Supplementary Fig. 1). These results show that E-selectin, but not P-selectin, acts in the bone marrow to accelerate HSC turnover.

Slower HSC cycling *in vivo* would suggest increased quiescence and greater self-renewal potential. We confirmed this by three independent assays: cell-cycle analysis, hydroxyurea S-phase suicide assay and rhodamine 123 (Rho) efflux. Cell-cycle analyses using an antibody to Ki-67, a nuclear marker of cell cycling, showed that 30% more HSCs were quiescent (in the G0 phase) in *Sele*^{-/-} mice compared to WT mice (Fig. 1d,e). We confirmed this result using the hydroxyurea *in vivo* suicide assay²⁰.

¹Stem Cells and Cancer Group, Mater Medical Research Institute, South Brisbane, Queensland, Australia. ²Stem Cell Biology Group, Mater Medical Research Institute, South Brisbane, Queensland, Australia. ³University of Queensland, School of Medicine, Brisbane, Queensland, Australia. ⁴GlycoMimetics Inc., Gaithersburg, Maryland, USA. Correspondence should be addressed to I.G.W. (iwinkler@mmri.mater.org.au) or J.-P.L. (jplevesque@mmri.mater.org.au).

Received 12 June; accepted 12 September; published online 21 October 2012; doi:10.1038/nm.2969

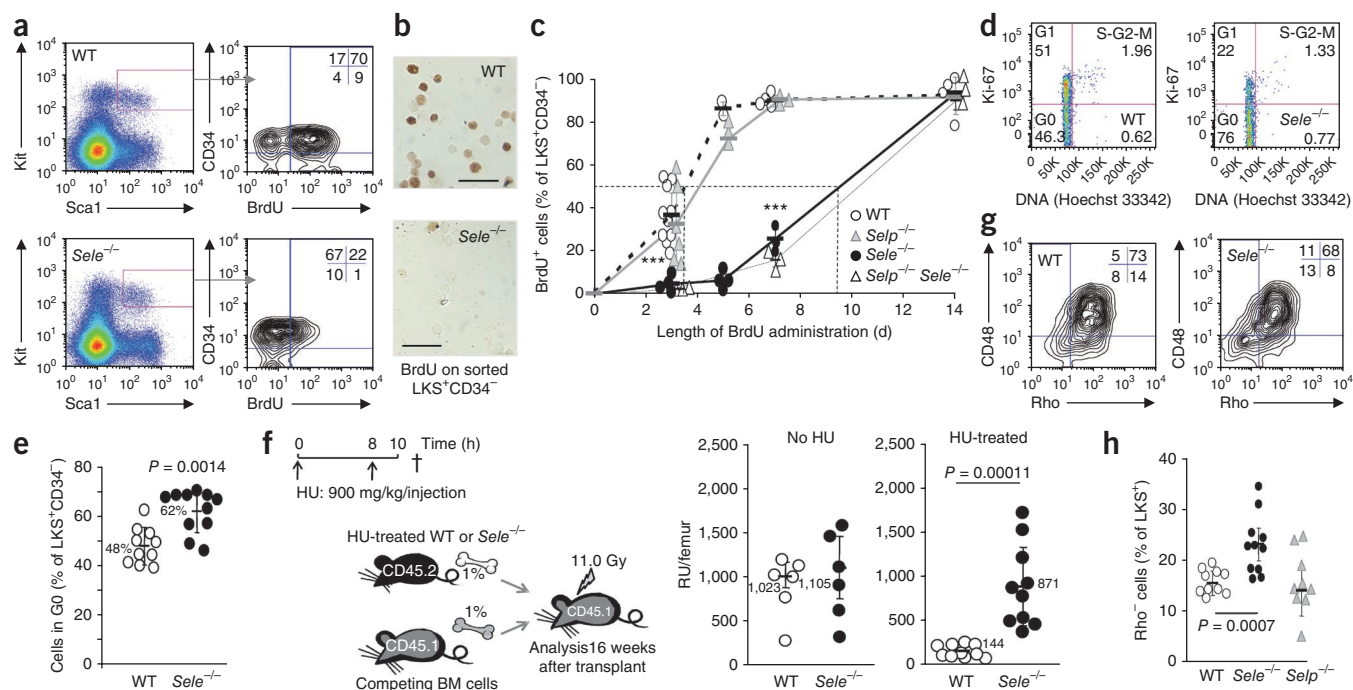


Figure 1 HSC quiescence is increased in E-selectin knockout (*Sele*^{-/-}) mice. **(a–c)** HSC turnover measured by BrdU incorporation in mice of the indicated genotypes continuously administered BrdU. At set periods of time, the percentage of BrdU incorporation in phenotypic HSCs was measured. **(a)** Dot plot showing the LKS⁺ gate within Lin⁻ bone marrow cells (left). BrdU after 3 d of incorporation and CD34 expression on gated LKS⁺ cells from representative mice (right). Inserted quadrants show percentages of cells in each quadrant of the dot plots. **(b)** Cytospins of sorted HSCs (LKS⁺CD34⁻) stained for BrdU incorporation after 5 d of BrdU administration. Scale bar, 50 μ m. **(c)** Percentage of bone marrow LKS⁺CD34⁻ HSCs that incorporated BrdU over time. Data are pooled from four separate experiments. ****P* < 0.001. **(d,e)** Cell-cycle analysis of LKS⁺CD34⁻ HSCs. **(d)** Typical dot plots of DNA content (Hoechst 33342) plotted versus Ki-67 nuclear antigen staining. The cell-cycle phases were defined as G0 (Ki-67⁻ and 2*n* DNA), G1 (Ki-67⁺ and 2*n* DNA) and S-G2-M (Ki-67⁺ and DNA >2*n*). **(e)** Percentage of LKS⁺CD34⁻ HSC in phase G0 (quiescence). **(f)** HSC quiescence in *Sele*^{-/-} and WT mice as measured by hydroxyurea (HU) *in vivo* suicide assay. Data shows the number of surviving reconstituting units (RU) per femur after injection with HU or no HU control. **(g,h)** Rhodamine efflux by HSCs. **(g)** Contour plot showing Rho efflux and CD48 staining on gated bone marrow LKS⁺ cells from representative mice. **(h)** Percentage of bone marrow LKS⁺ cell able to efflux Rho. Data are pooled from three separate experiments. Each symbol in **c,e,f** and **h** represents data for one mouse. All statistical significance was calculated by nonparametric Mann-Whitney test. All data are shown as the mean \pm s.d.

We injected hydroxyurea, an S phase-specific cytotoxic drug, into *Sele*^{-/-} or WT mice and then tested the bone marrow of these mice in long-term competitive repopulation (LT-CR) transplant assays to quantify the number of surviving HSCs. We found sixfold more surviving HSCs (expressed as reconstituting units²¹ per femur) in *Sele*^{-/-} compared to WT mice (**Fig. 1f**), confirming that a higher frequency of HSCs are quiescent when E-selectin is absent. Lastly, we measured Rho fluorescence to assess HSC numbers. Rho is a vital fluorescent dye effluxed by long-term repopulating HSCs with highest engraftment potential, similarly to Hoechst 33342 dye efflux by side-population cells²². The amount of Rho efflux was higher in HSCs from *Sele*^{-/-} mice compared to those from WT or *Selp*^{-/-} mice (**Fig. 1g,h**). Collectively these data confirm that E-selectin at the vascular niche induces HSC cycling.

Despite differences in HSC quiescence, the total number of HSCs per femur was not significantly different between *Sele*^{-/-} and WT mice, as measured by either limiting dilution LT-CR transplant assay or phenotypic analysis (**Supplementary Fig. 2**). This result shows that the effects of an E-selectin-deficient microenvironment on HSCs are qualitative (a greater proportion of HSCs being quiescent with heightened self renewal), not quantitative.

HSC proliferation induced by E-selectin is cell extrinsic

To confirm that the increased HSC quiescence in *Sele*^{-/-} mice is extrinsic to the HSCs (that is, microenvironmentally mediated), we generated fetal liver transplantation chimeras using fetal liver cells

from WT and *Sele*^{-/-} embryos and established long-term chimerism after transplantation into WT or *Sele*^{-/-} adult recipients. When transplanted into *Sele*^{-/-} recipients, WT HSCs showed 2.5-fold less turnover. In contrast, both WT and *Sele*^{-/-} HSCs showed normal turnover when transplanted into WT recipients (**Fig. 2**).

We next confirmed that, within the bone marrow, E-selectin is expressed exclusively by endothelial cells. We detected E-selectin RNA transcripts only in sorted bone marrow endothelial cells and not in any other hematopoietic or stromal cell populations tested (**Fig. 3a**). Overall, the amount of E-selectin mRNA was 16-fold higher in the bone marrow endosteal region as compared to the central bone marrow (**Fig. 3b**). Flow cytometry showed a similar enrichment of E-selectin-expressing endothelial cells in the endosteal region as compared to the central bone marrow (**Fig. 3c**), suggesting that the vasculature expressing E-selectin is enriched near the interface with bone. Furthermore, the number of E-selectin-positive endothelial cells increased 18-fold at the endosteum during the recovery phase from irradiation, when surviving HSCs must cycle to regenerate hematopoiesis (**Supplementary Fig. 3**). Together these data confirm that E-selectin expressed by endothelial cells at the HSC vascular niche accelerates HSC proliferation, and that this effect is extrinsically mediated by the bone marrow microenvironment.

Absence of E-selectin enhances HSC chemoresistance

Bone marrow suppression and life-threatening neutropenia can follow cytotoxic chemotherapy, and direct chemotherapy-induced damage

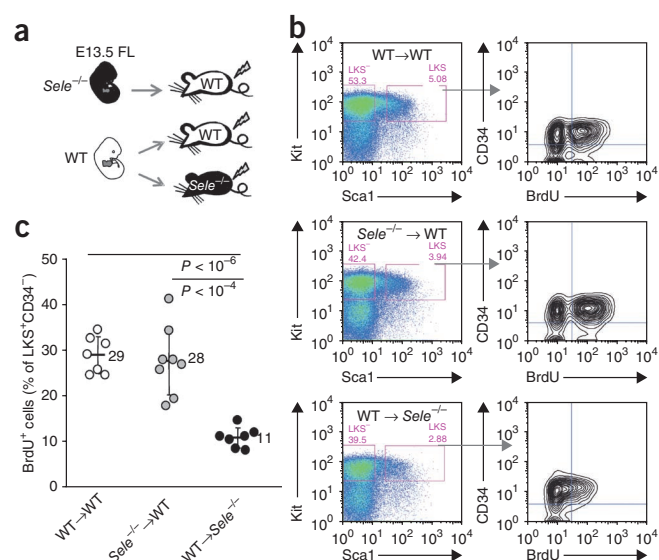
Figure 2 The effect of E-selectin on HSC turnover is mediated by the bone marrow microenvironment. **(a)** Model showing the establishment of transplantation chimeras using fetal liver cells from WT C57BL/6 or *Sele*^{-/-} embryos at embryonic day 13.5 (E13.5 FL) that were transplanted into lethally irradiated WT or *Sele*^{-/-} adult recipients. HSC turnover in these transplantation chimeras was tested 20 weeks after transplant, at which time they were treated with BrdU for 3 d. **(b)** Flow cytometry dot plot gating for LKS⁺ cells (left) and contour plots of BrdU incorporation and CD34 expression in gated LKS⁺ cells (right). **(c)** Percentage of bone marrow LKS⁺CD34⁻ HSCs that incorporated BrdU. Each dot represents a single mouse. Bars are the mean \pm s.d. All statistical significance was calculated by nonparametric Mann-Whitney test.

to HSCs is a contributing factor. Although HSCs can undergo self renewal, high-dose or repeated rounds of chemotherapy or irradiation can eventually exhaust the self-renewal capacity of the HSC pool, leading to prolonged bone marrow suppression and cytopenia. To test whether the relatively quiescent HSCs in *Sele*^{-/-} mice are more resistant to chemotherapy, we explored several models, including HSC survival after a single round of treatment with the antimetabolite 5-fluorouracil (5-FU) or repeated rounds of treatment with the alkylating agent cyclophosphamide (CYP), which also has immunomodulatory properties. We intraperitoneally administered each of these two cytotoxic drugs to WT and *Sele*^{-/-} mice and determined the number of surviving HSCs by LT-CR transplant assays. Indeed, 2.6-fold more HSCs, measured as reconstitution units (RU) per femur, survived a single injection of 5-FU in *Sele*^{-/-} mice (356 ± 123 (mean \pm s.d.) RU per femur) compared to WT mice (133 ± 57 RU per femur; **Fig. 4a**). This difference was more pronounced when the mice were treated with four rounds of CYP (one round every 2 weeks): HSCs in *Sele*^{-/-} mice showed an almost eight-fold greater survival compared to those in WT mice (1 in 52 of the initial reconstitution units per femur survived in WT mice compared to 1 in 9 in *Sele*^{-/-} mice) (**Fig. 4a**).

To test whether these effects on HSC survival would result in enhanced survival of the mice, we intraperitoneally administered 5-FU once every 10 d (150 mg per kg body weight) to cohorts of WT or *Sele*^{-/-} mice and monitored them for survival. In this assay, *Sele*^{-/-} mice showed significantly more resistance to repeated rounds of chemotherapy, with a median survival time exceeding 140 d, compared to a median survival time of 58 d in WT mice (**Fig. 4b**).

Faster blood recovery after irradiation of *Sele*^{-/-} mice

We next investigated whether peripheral leukocyte counts would also recover faster after stress in *Sele*^{-/-} mice. Intensive high-dose chemotherapy in human patients typically results in prolonged leukopenia with pronounced neutropenia. Mice, however, showed only a short drop



in the number of blood leukocytes after cytotoxic injection (**Fig. 5**). In contrast, we found that 9.0 Gy split-dose irradiation was not lethal in C57BL/6 mice but did induce prolonged leucopenia; under these conditions, WT mice required 28 d for their blood leukocyte numbers to return to the minimum normal threshold of 4,000 blood leukocytes per microliter. Blood leukocyte recovery was significantly accelerated in *Sele*^{-/-} mice after irradiation (**Fig. 4c**).

E-selectin antagonist also increases HSC chemoresistance

To be clinically useful, the benefits of enhanced HSC chemoresistance and faster leukocyte recovery after treatment need to be achievable by transient administration of an E-selectin antagonist. GMI-1070 is a small synthetic glycomimetic that blocks binding of E-selectin to its receptors²³. GMI-1070 has >50-fold higher selectivity for E-selectin than P- or L-selectin and is currently in phase 2 clinical trials for a separate indication, sickle-cell crisis²³.

We intraperitoneally administered GMI-1070 or saline to WT mice for 18–25 d and analyzed its effects on HSCs. We used a long period of GMI-1070 administration (bi-daily for 18–25 d), as recent studies have suggested that true HSCs cycle very infrequently in bone marrow, once every 35 d or more^{24,25}; thus, a prolonged period of drug administration may be needed to alter HSC turnover. Administration of GMI-1070 to WT mice delayed HSC cycling, with 37% less BrdU incorporation after a 3 d BrdU pulse (**Fig. 5a**), and increased the proportion of Rho-effluxing HSCs 44% compared to saline-administered controls (**Fig. 5a**). Therefore GMI-1070 was efficacious at reducing

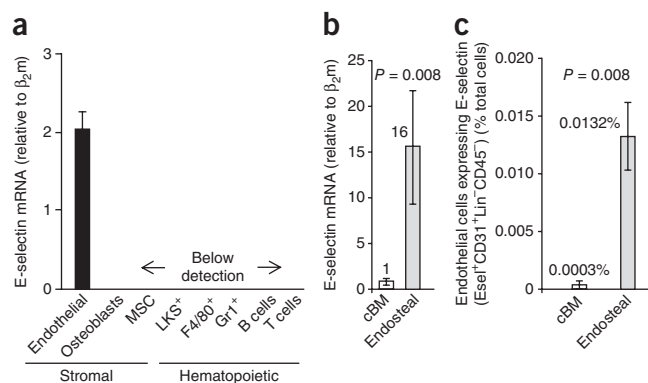


Figure 3 E-selectin-expressing endothelial cells are enriched in the endosteal region. **(a)** E-selectin mRNA expression relative to β_2 -microglobulin (β_2m) in the specified bone marrow cell populations sorted from WT mice and subjected to qRT-PCR. MSC, mesenchymal stromal cells. Data are the mean \pm s.d. **(b)** E-selectin mRNA expression relative to β_2 -microglobulin (β_2m) in RNA extracts from central bone marrow (cBM) and endosteal regions of the femur. Data are mean \pm s.d. from 3–4 mice per group. The data were normalized such that E-selectin mRNA expression in cBM was set to a value of 1. **(c)** The frequency of CD45⁺Lin⁻CD31⁺ endothelial cells expressing E-selectin (Esel), as determined by flow cytometry of bone marrow cells collected from central bone marrow and endosteum stained with mouse E-selectin-specific antibody. Data are mean \pm s.d. from four mice per group. All statistical significance was calculated by nonparametric Mann-Whitney test.

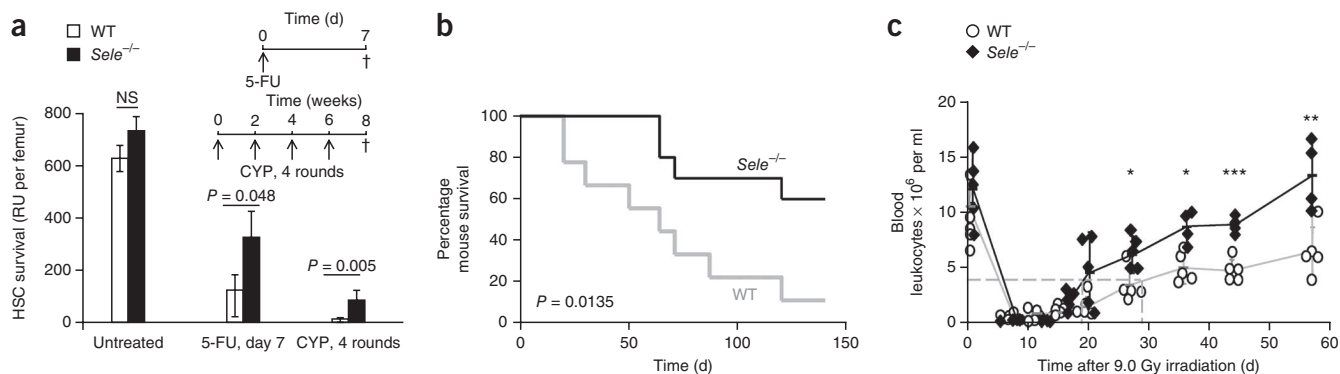


Figure 4 HSCs from *Sele*^{-/-} mice are chemoresistant and radioresistant. **(a)** Long-term reconstitution units (RU) 16 weeks after transplant in competitive repopulation transplant assays performed using bone marrow from donor WT or *Sele*^{-/-} mice, either untreated, after 7 d of treatment with a single dose of 5-FU or after treatment with four rounds of CYP. NS, not significant. Data are the mean \pm s.d. **(b)** Mouse survival in mice injected with 5-FU once every 10 d. **(c)** Blood leukocyte recovery in WT and *Sele*^{-/-} mice irradiated with 9.0 Gy. Each dot represents data for a single mouse. Bars are the mean \pm s.d. for each time point. * $P < 0.05$, ** $P < 0.01$, *** $P < 0.001$. All statistical significance was calculated by nonparametric Mann-Whitney test.

HSC proliferation despite the fact that GMI-1070 is bioactive for only 2 h in the serum after each bi-daily injection (when at a serum concentration of $>10 \mu\text{g ml}^{-1}$) (data not shown).

Although pretreatment with the E-selectin antagonist induced HSC quiescence, it did not increase HSC number per femur by either phenotypic analysis or LT-CR transplant assay in primary recipients (**Fig. 5b**). To further explore whether HSC self renewal was affected, we performed serial bone marrow transplantations. Serial transplantation is used to rapidly age HSCs, as extensive HSC self renewal is required to repopulate the whole hematopoietic system in each successive recipient. The use of serial bone marrow transplantation in the mouse mimics the gradual decline in HSC function over a lifetime in transplanted patients. When donor mice had been pretreated with saline, blood chimerism declined with each serial transplant, consistent with a gradual decline in HSC function, as previously reported²⁶. In sharp contrast, there was a steady increase

in reconstitution potential when the donor bone marrow was derived from mice pretreated with GMI-1070 (**Fig. 5b**). In tertiary transplant recipients, the number of reconstitution units per femur was 3.3-fold higher if the original donor had been pretreated for 25 d with GMI-1070 ($1,036 \pm 261$ compared to 309 ± 143 CD45.2⁺ RU per femur for saline-injected donors). These results show that transient pretreatment with the E-selectin antagonist *in vivo* significantly increases the self-renewal capacity of HSCs.

HSC quiescence may confer resistance to cytotoxic chemotherapy or radiotherapy. Indeed, when donor mice were administered a single dose of 5-FU and bone marrow transplanted in an LT-CR assay, we found that 2.9-fold more HSC survived if 5-FU donors had also been pretreated with GMI-1070 compared to 5-FU alone (**Fig. 5c**). Thus, transient administration of an E-selectin antagonist almost exactly mimics the increased HSC chemoresistance of *Sele*^{-/-} mice (**Fig. 4a**).

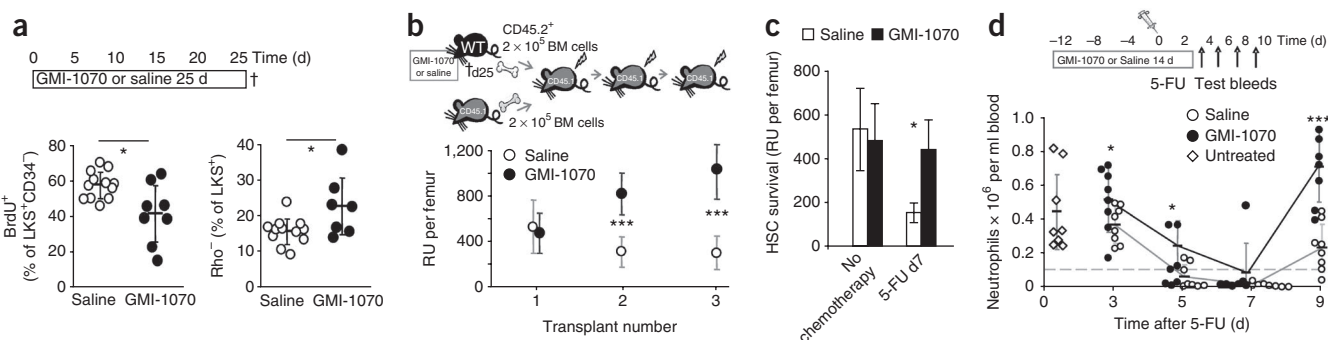


Figure 5 Administration of a small, synthetic E-selectin antagonist enhances HSC quiescence, chemoresistance, self-renewal capacity and blood leukocyte recovery after chemotherapy. **(a)** Diagram showing the timecourse of the experiment in which WT mice were administered the E-selectin antagonist GMI-1070 or saline for 18–25 d (top). Percentage of BrdU incorporation in gated bone marrow LKS⁺CD34⁻ HSCs (bottom left) and percentage of gated bone marrow LKS⁺ cells able to efflux Rho (Rho⁻) (bottom right). Data were pooled from two independent experiments. **(b)** The number of long-term competitive reconstitution units (RU) per CD45.2⁺ donor femur in a serial-transplantation assay in which 200,000 CD45.2⁺ bone marrow (BM) cells from GMI-1070-treated or saline-treated mice were transplanted into lethally irradiated congenic recipients together with an equal number of competing CD45.1⁺ bone marrow cells. At 25 weeks after primary transplants, 10% of the pooled femoral bone marrow was transplanted into secondary and then tertiary recipients each at 16 weeks after transplant. Data are the mean \pm s.d. $n = 8$ –10 recipients per group. **(c)** HSC survival measured by competitive long-term reconstitution assays 7 d after a single injection of 5-FU or saline in donor mice performed using pooled bone marrow from mice pretreated with GMI-1070 or saline. One percent of the femoral bone marrow was injected into recipients together with 200,000 congenic competing bone marrow cells. Data are mean \pm s.d. of the calculated number of long-term reconstitution units per femur. There were four donors and eight recipients per treatment group. **(d)** Blood CD11b⁺Gr1^{bright} neutrophil recovery measured by flow cytometry in GMI-1070-pretreated or control mice administered a single dose of 5-FU, as indicated. * $P < 0.05$, *** $P < 0.001$. Each symbol in **a** and **d** represents data from a single mouse, and all data are the mean \pm s.d. All statistical significance was calculated by nonparametric Mann-Whitney test.

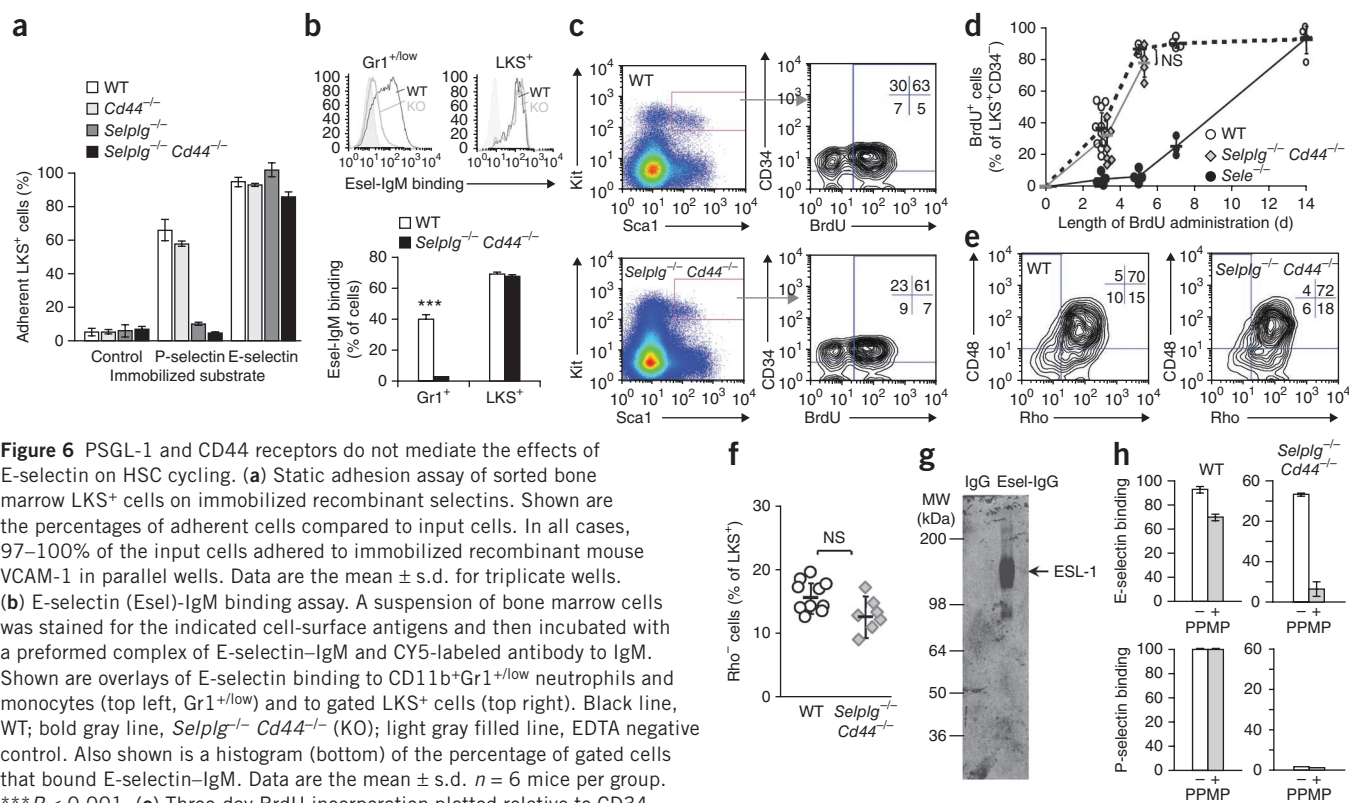


Figure 6 PSGL-1 and CD44 receptors do not mediate the effects of E-selectin on HSC cycling. **(a)** Static adhesion assay of sorted bone marrow LKS⁺ cells on immobilized recombinant selectins. Shown are the percentages of adherent cells compared to input cells. In all cases, 97–100% of the input cells adhered to immobilized recombinant mouse VCAM-1 in parallel wells. Data are the mean \pm s.d. for triplicate wells. **(b)** E-selectin (Esel)-IgM binding assay. A suspension of bone marrow cells was stained for the indicated cell-surface antigens and then incubated with a preformed complex of E-selectin-IgM and CY5-labeled antibody to IgM. Shown are overlays of E-selectin binding to CD11b⁺Gr1^{+/low} neutrophils and monocytes (top left, Gr1^{+/low}) and to gated LKS⁺ cells (top right). Black line, WT; bold gray line, *Selplg*^{-/-} *Cd44*^{-/-} (KO); light gray filled line, EDTA negative control. Also shown is a histogram (bottom) of the percentage of gated cells that bound E-selectin-IgM. Data are the mean \pm s.d. $n = 6$ mice per group. *** $P < 0.001$. **(c)** Three-day BrdU incorporation plotted relative to CD34 expression in gated LKS⁺ cells in WT and *Selplg*^{-/-} *Cd44*^{-/-} mice. Inserted quadrants show percentages of cells in each quadrant of the dot plots. **(d)** Timecourse of BrdU incorporation in gated bone marrow LKS⁺CD34⁻ cells. Bars are the mean \pm s.d. NS, not significant. **(e)** Rho efflux by HSCs. Contour plot showing Rho efflux plotted against CD48 staining on gated bone marrow LKS⁺ cells from representative WT and *Selplg*^{-/-} *Cd44*^{-/-} mice. **(f)** Percentage of bone marrow LKS⁺ cells able to efflux Rho. **(g)** E-selectin pulldown experiments. Lysates of Lin⁻Kit⁺ cells from *Selplg*^{-/-} *Cd44*^{-/-} mice were incubated with recombinant mouse E-selectin-huIgG1-Fc (Esel-IgG) or control (IgG)-coated beads, pulled down, eluted with EDTA and western blotted with a rabbit antibody to ESL-1. MW, molecular weight. **(h)** Binding of LKS⁺ cells from WT and *Selplg*^{-/-} *Cd44*^{-/-} mice to recombinant human E-selectin-IgM (top histograms) and P-selectin-IgM (bottom histograms) after an overnight incubation with or without PPMP, as measured by flow cytometry. Data are the mean \pm s.d. (triplicate wells, three repeats). Each symbol in **d** and **f** represents data from a single mouse. All statistical significance was determined by nonparametric Mann-Whitney test.

Short-term administration of GMI-1070 in mice also accelerated the recovery of blood neutrophils after 5-FU treatment (Fig. 5d). Therefore, transient pretreatment with an E-selectin antagonist not only increases the proportion of HSCs that are able to survive chemotherapy but also accelerates blood leukocyte recovery afterward.

Noncanonical E-selectin ligands mediate HSC proliferation

We have previously demonstrated that adhesion of human and mouse HSPCs to E- and P-selectin alters HSPC behavior *in vitro*^{27,28}. P-selectin glycoprotein ligand-1 (PSGL-1, also called CD162), the best-characterized selectin ligand, binds to both P- and E-selectin and is expressed by HSPCs, as well as by mature myeloid cells^{27–30}. However, absence of PSGL-1 did not prevent LKS⁺ HSPC adherence to E-selectin (Fig. 6a,b), even though the adhesion of mature Gr1⁺ myeloid cells to E-selectin was abrogated (Fig. 6b). Similarly, the absence of both PSGL-1 (*Selplg*^{-/-}) and the sialylated CD44 glycoform HCELL (*Cd44*^{-/-}), another canonical E-selectin ligand expressed by HSPCs and mature leukocytes^{30,31}, did not prevent HSPC binding to E-selectin in static-adhesion and flow cytometry-based assays (Fig. 6a,b). Furthermore, HSCs from *Selplg*^{-/-} *Cd44*^{-/-} mice incorporated BrdU at the same rate as did HSCs from WT mice (Fig. 6c,d) and did not show a significant difference in the number of Rho-negative cells (Fig. 6e,f), indicating that noncanonical ligands on HSCs mediate E-selectin-induced HSC proliferation.

To characterize E-selectin ligands on HSPCs, we used E-selectin-coated magnetic beads in pulldown experiments with lysates of Lin⁻Kit⁺ HSPCs from *Selplg*^{-/-} *Cd44*^{-/-} mice and looked for the presence of candidate E-selectin ligands by western blotting. Antibodies to CD43, endoglycan or CD147 (ref. 32) did not detect these candidate E-selectin ligands in pulldowns from HSPC extracts (data not shown). However, we did detect E-selectin ligand-1 (ESL-1), which most likely forms part of the E-selectin ligand signaling complex^{33–35} (Fig. 6g). We did not detect any other candidate E-selectin ligands, such as CD65 (by flow cytometry) or death receptor 3 (ref. 36) (by quantitative RT-PCR (qRT-PCR)) on LKS⁺ HSPCs.

Human neutrophils express both glycoprotein and glycosphingolipid E-selectin ligands³⁷. We next investigated whether mouse HSCs also express E-selectin-binding cell-surface glycosphingolipid ligands. We incubated mouse bone marrow HSPCs overnight in the presence of 18 μ M 1-phenyl-2-palmitoyl-3-morpholino-1-propanol (PPMP), a potent inhibitor of the glucosylceramide synthetase that is involved in the synthesis of glycosphingolipids³⁸. PPMP treatment reduced E-selectin binding by 88% in *Selplg*^{-/-} *Cd44*^{-/-} HSPCs and 30% in WT HSPCs (Fig. 6h). PSGL-1 glycoprotein binding to P-selectin was unaltered by PPMP treatment, showing the specificity of this treatment for glycosphingolipid ligands (Fig. 6h).

Together these results suggest that, in the absence of both PSGL-1 and CD44/HCELL, glycosphingolipids are major E-selectin ligands

on mouse HSPCs. Furthermore, as cell-surface glycosphingolipids are reported to be potent adhesion and signaling molecules (forming the glycosynapse^{39,40}), such glycosphingolipids may be involved in transducing E-selectin-mediated signaling from endothelial cells forming the vascular niche to HSCs.

DISCUSSION

Here we report that E-selectin expressed on the bone marrow vasculature is a potent driver of HSC proliferation *in vivo*. Furthermore, we found that transient administration of a small synthetic E-selectin antagonist blocks proliferative signaling by the vascular HSC niche, promoting HSC quiescence, HSC self renewal and increased survival after treatment with chemotherapeutic agents *in vivo*.

Environmental cues are crucial regulators of normal and malignant stem-cell behavior. Far from being homogenous, bone marrow tissue contains a mosaic of microenvironments, each of which provides a unique set of instructions regulating or reinforcing cell fate. The most potent and quiescent HSCs are enriched near osteoblasts lining the endosteal bone surface^{1–4,24} and in poorly perfused areas of the bone marrow⁴¹, leading to the hypothesis that unique factors and cues at these niches actively maintain HSC quiescence and self-renewal capacity. By inference, HSCs located outside these specialized niches may commit to hematopoietic lineages and lose stem-cell potential in the absence of osteoblastic cues. We now show that the adhesion molecule E-selectin is a crucial component of the vascular HSC niche that actively induces HSC proliferation. E-selectin deficiency or antagonism leads to HSC quiescence, a greater capacity to self renew and enhanced chemoresistance. Our findings challenge the current assumption that factors unique to the osteoblastic niche alone maintain HSC dormancy and self renewal and are supported by recent evidence showing a key role for Kit ligand expressed by endothelial cells in HSC maintenance¹⁰. Indeed it seems that in the absence of a specific E-selectin-mediated proliferative signal, greater numbers of HSC remain quiescent.

That HSC proliferation seems to be regulated by E-selectin but not P-selectin is surprising, as both endothelial selectins are largely redundant in function in the periphery, and *Sele*^{-/-} mice have no obvious phenotype and have normal blood indices^{42,43}. Intravital imaging studies on mouse calvariae have suggested that E-selectin is expressed mainly on bone marrow sinusoidal vasculature, whereas P-selectin is present on larger blood vessels¹⁶. Thus, it seems that these two endothelial selectins may be expressed in distinct, possibly nonoverlapping locations in the bone marrow and have distinct functional roles in this tissue. Furthermore, we found that the expression of E-selectin is greatly increased during the recovery phase after irradiation when HSCs divide to reconstitute hematopoiesis, supporting the notion that E-selectin promotes HSC proliferation in regenerating or inflamed bone marrow.

The identity of the E-selectin ligand involved in regulating HSC cycling in the bone marrow remains uncertain. None of the canonical E-selectin ligands tested had an effect on HSCs; however, the involvement of ESL-1 cannot be excluded, as we detected it in E-selectin pull-downs from HPSC cell lysates. ESL-1 is a glycoprotein of the Golgi apparatus, but in cell culture, its expression may be redirected to the cell-surface plasma membrane after post-translational modifications, such as the addition of a glycosylphosphatidylinositol anchor^{44,45}. Notably, inhibition of sphingolipid glycosylation reduced the E-selectin binding of *Selplg*^{-/-} *Cd44*^{-/-} HSCs by 88%, suggesting that glycosphingolipids may also be important E-selectin ligands on HSCs. To our knowledge, glycosphingolipid E-selectin ligands have

not previously been reported on normal adult stem cells. It is tempting to speculate that such glycosphingolipid E-selectin ligands might be involved in cell signaling only when HSCs are already in close physical contact with E-selectin at the vascular niche.

Aberrant glycosylation is characteristic of many tumor cells and is a frequent early marker of oncogenic transformation⁴⁶. The *de novo* expression of E-selectin ligands on tumor cells is thought to aid their homing and engraftment into the bone marrow^{47–49}. Our findings suggest that the acquisition of E-selectin ligands by tumor cells may also influence subsequent tumor cell proliferation and tumor growth.

Finally, chemotherapy-induced bone marrow suppression remains a clinical problem. Reducing the myelosuppressive effect of chemotherapy could result in less infection and less of a requirement for blood product and hospital support. Our study of how the vascular niche regulates stem-cell behavior suggests a new approach to alleviate these potentially life-threatening complications of chemotherapy.

METHODS

Methods and any associated references are available in the [online version of the paper](#).

Note: Supplementary information is available in the [online version of the paper](#).

ACKNOWLEDGMENTS

The authors wish to thank R. Wadley for assistance with cell sorting, P. Frenette (Albert Einstein College of Medicine, New York) for providing selectin knockout mice, B. Furie (Beth Israel Deaconess Medical Center, Harvard Medical School, Boston) for *Selplg*^{-/-} mice, T. Mak (Ontario Cancer Institute, Toronto) for *Cd44*^{-/-} mice, D. Vestweber (Max Planck Institute of Molecular Biomedicine, Münster, Germany) for antibody to ESL-1, K. Snapp (Northwestern University, Chicago) for selectin-IgM constructs and L. Purton, C. Walkley and C. Bonder for helpful discussions. This work was supported by project grants 350406 and 543706 (I.G.W. and J.-P.L.) and Career Development Fellowships 488817 and APP1033736 (I.G.W.) from the National Health and Medical Research Council of Australia, a Senior Research Fellowship from the Cancer Council of Queensland (J.-P.L.) and a research contract with GlycoMimetics Inc to generate the data in **Figure 5**.

AUTHOR CONTRIBUTIONS

I.G.W. initiated, conceived of, designed and supervised research, wrote the manuscript, performed experiments and analyzed data. V.B., B.N., R.N.J. and C.E.F. performed experiments and analyzed data. J.T.P. and J.L.M. contributed vital new reagents and commented on the research direction. J.-P.L. initiated the study, supervised research direction and experiments, performed some experiments and edited the manuscript. All authors discussed and commented on the manuscript.

COMPETING FINANCIAL INTERESTS

The authors declare competing financial interests: details are available in the [online version of the paper](#).

Published online at <http://www.nature.com/doi/10.1038/nm.2969>.

Reprints and permissions information is available online at <http://www.nature.com/reprints/index.html>.

1. Arai, F. *et al.* Tie2/angiopoietin-1 signaling regulates hematopoietic stem cell quiescence in the bone marrow niche. *Cell* **118**, 149–161 (2004).
2. Xie, Y. *et al.* Detection of functional haematopoietic stem cell niche using real-time imaging. *Nature* **457**, 97–101 (2009).
3. Köhler, A. *et al.* Altered cellular dynamics and endosteal location of aged early hematopoietic progenitor cells revealed by time-lapse intravital imaging in long bones. *Blood* **114**, 290–298 (2009).
4. Lo Celso, C. *et al.* Live-animal tracking of individual haematopoietic stem/progenitor cells in their niche. *Nature* **457**, 92–96 (2009).
5. Lévesque, J.P., Helwani, F.M. & Winkler, I.G. The endosteal 'osteoblastic' niche and its role in hematopoietic stem cell homing and mobilization. *Leukemia* **24**, 1979–1992 (2010).
6. Kiel, M.J. *et al.* SLAM family receptors distinguish hematopoietic stem and progenitor cells and reveal endothelial niches for stem cells. *Cell* **121**, 1109–1121 (2005).
7. Sugiyama, T., Kohara, H., Noda, M. & Nagasawa, T. Maintenance of the hematopoietic stem cell pool by CXCL12-CXCR4 chemokine signaling in bone marrow stromal cell niches. *Immunity* **25**, 977–988 (2006).

8. Méndez-Ferrer, S. *et al.* Mesenchymal and haematopoietic stem cells form a unique bone marrow niche. *Nature* **466**, 829–834 (2010).
9. Butler, J.M. *et al.* Endothelial cells are essential for the self-renewal and repopulation of Notch-dependent hematopoietic stem cells. *Cell Stem Cell* **6**, 251–264 (2010).
10. Ding, L., Saunders, T.L., Enikolopov, G. & Morrison, S.J. Endothelial and perivascular cells maintain haematopoietic stem cells. *Nature* **481**, 457–462 (2012).
11. Kansas, G.S. Selectins and their ligands: current concepts and controversies. *Blood* **88**, 3259–3287 (1996).
12. Frenette, P.S., Mayadas, T.N., Rayburn, H., Hynes, R.O. & Wagner, D.D. Susceptibility to infection and altered hematopoiesis in mice deficient in both P- and E-selectins. *Cell* **84**, 563–574 (1996).
13. Maly, P. *et al.* The $\alpha(1,3)$ fucosyltransferase Fuc-TVII controls leukocyte trafficking through an essential role in L-, E-, and P-selectin ligand biosynthesis. *Cell* **86**, 643–653 (1996).
14. Jacobsen, K., Kravitz, J., Kincade, P.W. & Osmond, D.G. Adhesion receptors on bone marrow stromal cells: *in vivo* expression of vascular cell adhesion molecule-1 by reticular cells and sinusoidal endothelium in normal and γ -irradiated mice. *Blood* **87**, 73–82 (1996).
15. Schweitzer, K.M. *et al.* Constitutive expression of E-selectin and vascular cell adhesion molecule-1 on endothelial cells of hematopoietic tissues. *Am. J. Pathol.* **148**, 165–175 (1996).
16. Sipkins, D.A. *et al.* *In vivo* imaging of specialized bone marrow endothelial microdomains for tumour engraftment. *Nature* **435**, 969–973 (2005).
17. Hidalgo, A., Weiss, L.A. & Frenette, P.S. Functional selectin ligands mediating human CD34⁺ cell interactions with bone marrow endothelium are enhanced postnatally. *J. Clin. Invest.* **110**, 559–569 (2002).
18. Katayama, Y. *et al.* PSGL-1 participates in E-selectin-mediated progenitor homing to bone marrow: evidence for cooperation between E-selectin ligands and $\alpha 4$ integrin. *Blood* **102**, 2060–2067 (2003).
19. Osawa, M., Hanada, K., Hamada, H. & Nakauchi, H. Long-term lymphohematopoietic reconstitution by a single CD34-low/negative hematopoietic stem cell. *Science* **273**, 242–245 (1996).
20. Lord, B.I., Dexter, T.M., Clements, J.M., Hunter, M.A. & Gearing, A.J. Macrophage-inflammatory protein protects multipotent hematopoietic cells from the cytotoxic effects of hydroxyurea *in vivo*. *Blood* **79**, 2605–2609 (1992).
21. Purton, L.E. & Scadden, D.T. Limiting factors in murine hematopoietic stem cell assays. *Cell Stem Cell* **1**, 263–270 (2007).
22. Hüttmann, A., Liu, S.L., Boyd, A.W. & Li, C.L. Functional heterogeneity within rhodamine123(Io) Hoechst33342(Io/sp) primitive hematopoietic stem cells revealed by pyronin Y. *Exp. Hematol.* **29**, 1109–1116 (2001).
23. Chang, J. *et al.* GMI-1070, a novel pan-selectin antagonist, reverses acute vascular occlusions in sickle cell mice. *Blood* **116**, 1779–1786 (2010).
24. Wilson, A. *et al.* Hematopoietic stem cells reversibly switch from dormancy to self-renewal during homeostasis and repair. *Cell* **135**, 1118–1129 (2008).
25. Catlin, S.N., Busque, L., Gale, R.E., Guttrop, P. & Abkowitz, J.L. The replication rate of human hematopoietic stem cells *in vivo*. *Blood* **117**, 4460–4466 (2011).
26. Purton, L.E. *et al.* RAR γ is critical for maintaining a balance between hematopoietic stem cell self-renewal and differentiation. *J. Exp. Med.* **203**, 1283–1293 (2006).
27. Lévesque, J.P. *et al.* PSGL-1-mediated adhesion of human hematopoietic progenitors to P-selectin results in suppression of hematopoiesis. *Immunity* **11**, 369–378 (1999).
28. Winkler, I.G., Snapp, K.R., Simmons, P.J. & Levesque, J.-P. Adhesion to E-selectin promotes growth inhibition and apoptosis of human and murine hematopoietic progenitor cells independent of PSGL-1. *Blood* **103**, 1685–1692 (2004).
29. Eto, T., Winkler, I., Purton, L.E. & Levesque, J.P. Contrasting effects of P-selectin and E-selectin on the differentiation of murine hematopoietic progenitor cells. *Exp. Hematol.* **33**, 232–242 (2005).
30. Dimitroff, C.J., Lee, J.Y., Rafii, S., Fuhlbrigge, R.C. & Sackstein, R. CD44 is a major E-selectin ligand on human hematopoietic progenitor cells. *J. Cell Biol.* **153**, 1277–1286 (2001).
31. Katayama, Y., Hidalgo, A., Chang, J., Peired, A. & Frenette, P.S. CD44 is a physiological E-selectin ligand on neutrophils. *J. Exp. Med.* **201**, 1183–1189 (2005).
32. Zarbock, A., Ley, K., McEver, R.P. & Hidalgo, A. Leukocyte ligands for endothelial selectins: specialized glycoconjugates that mediate rolling and signaling under flow. *Blood* **118**, 6743–6751 (2011).
33. Hidalgo, A., Peired, A.J., Wild, M.K., Vestweber, D. & Frenette, P.S. Complete identification of E-selectin ligands on neutrophils reveals distinct functions of PSGL-1, ESL-1, and CD44. *Immunity* **26**, 477–489 (2007).
34. Zöllner, O. & Vestweber, D. The E-selectin ligand-1 is selectively activated in Chinese hamster ovary cells by the $\alpha(1,3)$ -fucosyltransferases IV and VII. *J. Biol. Chem.* **271**, 33002–33008 (1996).
35. Wild, M.K., Huang, M.C., Schulze-Horsell, U., van der Merwe, P.A. & Vestweber, D. Affinity, kinetics, and thermodynamics of E-selectin binding to E-selectin ligand-1. *J. Biol. Chem.* **276**, 31602–31612 (2001).
36. Gout, S., Morin, C., Houle, F. & Huot, J. Death receptor-3, a new E-Selectin counter-receptor that confers migration and survival advantages to colon carcinoma cells by triggering p38 and ERK MAPK activation. *Cancer Res.* **66**, 9117–9124 (2006).
37. Nimrichter, L. *et al.* E-selectin receptors on human leukocytes. *Blood* **112**, 3744–3752 (2008).
38. Sandvig, K., Garred, O., van Helvoort, A., van Meer, G. & van Deurs, B. Importance of glycolipid synthesis for butyric acid-induced sensitization to shiga toxin and intracellular sorting of toxin in A431 cells. *Mol. Biol. Cell* **7**, 1391–1404 (1996).
39. Todeschini, A.R., Dos Santos, J.N., Handa, K. & Hakomori, S.I. Ganglioside GM2-tetraspanin CD82 complex inhibits met and its cross-talk with integrins, providing a basis for control of cell motility through glycosynapse. *J. Biol. Chem.* **282**, 8123–8133 (2007).
40. Todeschini, A.R. & Hakomori, S. Functional role of glycosphingolipids and gangliosides in control of cell adhesion, motility and growth, through glycosynaptic microdomains. *Biochim. Biophys. Acta* **1780**, 421–433 (2008).
41. Winkler, I.G. *et al.* Positioning of bone marrow hematopoietic and stromal cells relative to blood flow *in vivo*: serially reconstituting hematopoietic stem cells reside in distinct nonperfused niches. *Blood* **116**, 375–385 (2010).
42. Labow, M.A. *et al.* Characterization of E-selectin-deficient mice: demonstration of overlapping function of the endothelial selectins. *Immunity* **1**, 709–720 (1994).
43. Kunkel, E.J. & Ley, K. Distinct phenotype of E-selectin-deficient mice: E-selectin is required for slow leukocyte rolling *in vivo*. *Circ. Res.* **79**, 1196–1204 (1996).
44. Steegmaier, M., Borges, E., Berger, J., Schwarz, H. & Vestweber, D. The E-selectin-ligand ESL-1 is located in the Golgi as well as on microvilli on the cell surface. *J. Cell Sci.* **110**, 687–694 (1997).
45. Miyaoka, Y. *et al.* Retention in the Golgi apparatus and expression on the cell surface of Cfr/Esl-1/Glg-1/MG-160 are regulated by two distinct mechanisms. *Biochem. J.* **440**, 33–41 (2011).
46. Hakomori, S. Tumor malignancy defined by aberrant glycosylation and sphingo(glyco)lipid metabolism. *Cancer Res.* **56**, 5309–5318 (1996).
47. Gout, S., Tremblay, P.L. & Huot, J. Selectins and selectin ligands in extravasation of cancer cells and organ selectivity of metastasis. *Clin. Exp. Metastasis* **25**, 335–344 (2008).
48. Tremblay, P.L., Auger, F.A. & Huot, J. Regulation of transendothelial migration of colon cancer cells by E-selectin-mediated activation of p38 and ERK MAP kinases. *Oncogene* **25**, 6563–6573 (2006).
49. Dimitroff, C.J. *et al.* Identification of leukocyte E-selectin ligands, P-selectin glycoprotein ligand-1 and E-selectin ligand-1, on human metastatic prostate tumor cells. *Cancer Res.* **65**, 5750–5760 (2005).

ONLINE METHODS

Mice, injections and sample preparation. All mouse experiments were approved by the University of Queensland animal experimentation ethics committee. WT (CD45.2⁺) C57BL/6 and congenic B6.SJL (CD45.1⁺) mice were purchased from the Animal Resource Centre, Perth, Australia. Knockout mice were donated by P. Frenette (*Sele*^{-/-}, *Selp*^{-/-} and *Sele*^{-/-} *Selp*^{-/-}), Bruce and Barbara Furie (*Selplg*^{-/-}), and T. Mak (*Cd44*^{-/-}). All mice had been backcrossed on a C57BL/6 background at least eight times. All mice were age and sex matched within an experiment. No differences between sexes were observed between experimental replicates. Transplantation recipients were females to reduce fighting.

BrdU was administered at 0.5 mg ml⁻¹ in drinking water changed twice weekly. 5-FU was injected at 150 mg per kg body weight intraperitoneally (i.p.) once or every 10 d; CYP was injected at 200 mg per kg body weight i.p. once every two weeks for a total of four rounds of injection. GMI-1070 from GlycoMimetics was administered i.p. at 50 mg per kg body weight per injection bi-daily.

After euthanasia, femurs were collected and flushed into ice-cold PBS plus 2% newborn calf serum (NCS) for the isolation of bone marrow cells. The empty femurs were flushed twice more in PBS then flushed with 1 ml TRIzol (Invitrogen) for endosteal RNA preparation⁵⁰ or with 1 mg ml⁻¹ collagenase 1 (Worthington) every 5 min at 37 °C for 30 min to dislodge endosteal cells, which were then used for flow cytometry^{51,52}.

Flow cytometry stains. All antibody dilutions and clone numbers are described in **Supplementary Table 1**. For Rho staining, bone marrow cells were resuspended at 1×10^6 ml⁻¹ in warm PBS plus 2% NCS containing 10 ng ml⁻¹ Rho (Invitrogen) and incubated for 20 min at 37 °C with agitation. Cells were then washed in warm PBS plus 2% NCS and allowed to efflux the dye for 15 min at 37 °C before washing on ice and staining with biotinylated lineage antibody cocktail (CD3e, CD5, B220, CD11b, Gr1 and Ter119) and biotinylated CD41 together with streptavidin (SAV) conjugated to peridinin chlorophyll protein complex (PerCP)-CY5.5, antibody to Sca1 conjugated to phycoerythrin (PE)-CY7, antibody to Kit conjugated to allophycocyanin (APC), CD48-PacificBlue and CD150-PE⁵³.

For BrdU staining, bone marrow cells were first enriched in Kit⁺ cells by magnetic-activated cell sorting (MACS) using mouse CD117 magnetic beads and an auto-MACS device (Miltenyi, Germany). Kit⁺ enriched cells were stained with biotinylated lineage plus CD41 antibody cocktail together with SAV-PerCP-CY5.5, antibody to Sca1-PE-CY7, antibody to Kit-APC-H7, CD48-PacificBlue, CD150-PE and CD34-FITC. In initial experiments, LKS⁺CD34⁻ cells were first sorted by fluorescence-activated cell sorting (FACS), spread on slides and then stained for BrdU incorporation. In later experiments, anti-BrdU staining was performed in suspension, and BrdU incorporation was analyzed by flow cytometry as previously described⁵³. Both methods used anti-BrdU kits from BD Pharmingen.

The cell cycle was analyzed on Kit⁺ MACS-enriched cells. Live cells were surface stained with CD48-PerCP-Cy5.5, antibodies to Sca1-PE-CY7, antibodies to Kit-APC-H7, CD34-e660 and CD150-PE and then fixed and permeabilized before staining with FITC-conjugated antibodies to Ki-67 and Hoechst 33342 (ref. 53).

For endothelial cell staining, recovered endosteal cells were stained with FITC-conjugated lineage cocktail, CD45-APC-Cy7, CD31-APC, Sca1-PE-CY7 and PE-conjugated rat antibodies to mouse E-selectin or isotype-matched control.

Mouse transplantations and blood recovery. In standard LT-CR transplant assays, 2×10^5 donor CD45.2⁺ bone marrow cells (unless otherwise specified) were mixed with 2×10^5 competing whole bone marrow cells from congenic B6.SJL CD45.1⁺ mice and injected retro-orbitally into lethally irradiated (11.0 Gy split dose) congenic CD45.1⁺ recipients, as previously described⁵⁴. For chemotherapy-treated mice, the equivalent of 1% of the femoral contents at 7 d after treatment with 5-FU, or 10% of the femoral contents at 14 d after four rounds of CYP treatment, was injected together with 2×10^5 congenic competing bone marrow cells in each irradiated recipient mouse. Mice were given Bactrim antibiotic in their drinking water for 2 weeks after transplantation.

Multilineage chimerism was measured by flow cytometry at 16–25 weeks after transplant and after staining of blood leukocytes with CD45.1-PE, CD45.2-APC,

CD11b-PE-CY7, B220-APC-CY7 and CD3e-FITC. The number of CD45.2⁺ reconstitution units (RU) injected per recipient mouse was calculated using the formula $(D \times C)/(100 - D)$, where D is the percentage of recipient blood leukocytes that are CD45.2⁺ at the 16-week test bleed, and C the number of competing CD45.1⁺ reconstitution units that were co-injected (in most cases $C = 2$, meaning that 2×10^5 competing bone marrow cells were injected). Reconstitution units per femur were then calculated. One RU is defined as the HSC content in 1×10^5 bone marrow cells²¹.

For serial transplants, primary recipients were euthanized 25 weeks after transplant, femoral bone marrow was harvested and pooled within each group, and the equivalent of 10% of the femoral content of one mouse ($\sim 2.5 \times 10^6$ bone marrow cells) was injected into each lethally irradiated congenic secondary recipient (eight recipients per group). Multilineage chimerism was measured 16 weeks after secondary and tertiary transplant.

In vivo hydroxyurea suicide assay. *Sele*^{-/-} and age-matched, sex-matched WT mice were injected twice (8 h apart) i.p. with 900 mg per kg body weight hydroxyurea²⁰. Bone marrow was harvested 2 h after the last hydroxyurea injection by crushing individual femurs in PBS plus 2% FCS. The equivalent of 1% of the bone marrow leukocytes from the femur of each *Sele*^{-/-} or WT mouse was mixed with 1% of the bone marrow leukocytes from the femurs of congenic B6.SJL (CD45.1⁺) untreated mice and transplanted into lethally irradiated B6.SJL recipients. Lineage chimerism was measured at 16 weeks after transplant.

Transplantation chimeras. Eight-week-old female *Sele*^{-/-} and WT mice were lethally irradiated with 11.0 Gy (in two split doses of 5.5 Gy 3–4 h apart). The next day, fetal livers were harvested at E13.5 from *Sele*^{-/-} and WT pregnant females and gently crushed with the back of a 5-ml syringe piston over a 40- μ m sieve in PBS plus 2% FCS. Fetal liver cells were pooled, washed once and resuspended in sterile saline for injection. Each lethally irradiated recipient received cells from one-third of a fetal liver injected retro-orbitally. BrdU incorporation was measured at 20 weeks after transplantation.

Blood recovery after irradiation. Mice were irradiated with a split dose of 9.0 Gy (two split doses of 4.5 Gy 3 h apart) and then allowed to recover. Mice were given Bactrim antibiotic in their drinking water until their blood counts recovered. A small amount of blood was collected from the tail vein at set time-points before and after irradiation and subjected to blood leukocyte counts using an automated hematological analyzer (Sysmex KX21).

E-selectin adhesion assays. For static adhesion assays, 96-well plates were coated with purified recombinant mouse VCAM-1, E-selectin- or P-selectin-human IgG1 (huIgG1)-Fc fusion proteins (R&D Systems)²⁸, washed and blocked with BSA. Sorted bone marrow LKS⁺ cells were labeled with 10 μ M calcein-AM²⁸ (Molecular Probes) and washed, and then 5,000 labeled cells were added to each of triplicate selectin- or control-coated wells. After gentle sedimentation by centrifugation, cells were left in contact with the coated surface for 20 min at 4 °C, washed four times, and the percentage of adherent cells was quantified as previously described²⁸.

For selectin binding in suspension, recombinant E-selectin-huIgM fusion protein supernatants were precomplexed with CY5-conjugated donkey F(ab)₂ antibody to human IgM (Jackson ImmunoResearch) for 1 h on ice as previously described³¹ and then added to bone marrow cells prestained on ice with biotinylated lineage markers (B220, CD3e and Ter119), SAV-AlexaFluor 700, Gr1-FITC, CD11b-PacificBlue, Sca1-PE-CY7 and Kit-PE in Fc block media containing 4 mM CaCl₂ or media containing EDTA as a negative nonbinding control. After 20 min on ice, cells were washed and analyzed by flow cytometry with 2 μ g ml⁻¹ 7-aminoactinomycin D to assess viability. In some experiments, bone marrow cells were enriched in Kit⁺ cells by MACS and cultured overnight in Iscove's Modified Dulbecco's Medium supplemented with 10% FCS and 50 ng ml⁻¹ recombinant mouse Kit ligand with or without 18 μ M PMP (Sigma) to block sphingolipid glycosylation before measurement of selectin-huIgM binding.

E-selectin receptor pull down and western blotting. Protein G-conjugated magnetic Dynabeads (Dyna) were loaded with recombinant mouse E-selectin-huIgG1-Fc fusion protein or purified human IgG overnight at 4 °C on a

rotator (1 µg protein per 10 µl beads). Loaded beads were extensively washed with HEPES-buffered saline containing 0.1% Triton X-100, 0.1% BSA, 4 mM CaCl₂ and 1 mM MgCl₂ by magnetic pelleting. Then, 5 × 10⁶ MACS-lineage depleted and MACS-Kit⁺ enriched bone marrow cells from *Selplg*^{-/-} *Cd44*^{-/-} mice were lysed on ice for 30 min in 1 ml HEPES-buffered saline containing 1% Triton X-100, 0.1% BSA, 4 mM CaCl₂, 1 mM MgCl₂, 200 µM phenylmethyl sulfonyl fluoride, 2 µg ml⁻¹ pepstatin A, 2 µg ml⁻¹ aprotinin, 5 µM leupeptin and 1 µg ml⁻¹ E64. Cells lysates were centrifuged at 13,000g for 10 min at 4 °C, the supernatant was collected and the lysates were precleared with naive protein G-conjugated beads for 30 min. Precleared cell lysates were then rotated for 30 min at 4 °C with 4 µg E-selectin-coated beads or control human IgG-coated beads. Beads were washed four times by magnetic pelleting. E-selectin-binding proteins were then eluted twice in 20 µl PBS plus 10 mM EDTA. Eluates were electrophoresed on an 8% polyacrylamide gel. After electrotransfer, nitrocellulose-coated nylon membranes were blocked and then incubated overnight with either 1/1,000 rabbit antibody to mouse ESL-1 serum (donated by D. Vestweber)⁴⁴, 1/500 biotinylated rat antibody to mouse CD43 (clones S7 and 1B11, BD Pharmingen and BioLegend), 1/500 rabbit antibody to PODXL2 (16383-1-AP, Proteintec) or 1/500 rabbit antibody to CD147 (ab70062, Abcam). Membranes were then washed and incubated with 1/10,000 IRDye800-conjugated donkey antibody to rabbit IgG (611-732-127, Rockland Immunochemicals) or streptavidin. Membranes were analyzed with an Odyssey Infrared Imaging System⁵⁵.

Cell sorting for RNA expression by qRT-PCR. Total central bone marrow and endosteal RNA were collected from individual mice using TRIzol as described in the sample preparation section above. RNA was also extracted from the following FACS-sorted bone marrow hematopoietic cell populations: HSPCs (LKS⁺), macrophages (F4/80⁺Gr1⁻CD11b⁺), neutrophils (Gr1⁺F4/80⁻CD11b⁺), B cells (B220⁺CD11b⁻) and T cells (CD3⁺CD11b⁻). For identifying stromal and endothelial cells, partially crushed bones were incubated with 3 mg ml⁻¹ type I collagenase for 40 min at 37 °C; released cells were MACS-depleted of lineage-positive (Lin⁺) cells and then stained as previously described⁵⁶. Bone marrow endothelial cells (Lin⁻CD45⁻CD31⁺), MSCs (Lin⁻CD45⁻CD31⁻Sca1⁺CD51⁺)

and osteoblastic cells (Lin⁻CD45⁻CD31⁻Sca1⁻CD51⁺) were sorted as previously validated⁵², and RNA was extracted. After DNase treatment and reverse transcription using random hexamers, real-time qRT-PCR with SYBR Green (ABI Systems) was performed according to the manufacturer's instructions using the following oligonucleotides: β₂-microglobulin (forward, 5'-TTCACCCCCACTGAGACTGAT-3'; reverse, 5'-GTCTTGGGCTCGGCCATA-3'), E-selectin (forward, 5'-GTCTAGCGCCTGGATGAAAG-3'; reverse, 5'-ATYGCCACCAGATGTGTGTA-3', where Y indicates either C or T) and death receptor 3 (forward, 5'-TGCCCAAAGGACACTACAT-3'; reverse, 5'-GCAGCGGGTACAGTCAGTC T-3'). A PCR from each sample before reverse transcription was also performed to confirm the absence of contaminating genomic DNA.

Statistical analyses. A nonparametric Mann-Whitney test was used for statistical analyses, except for the limiting dilution LT-RC assay, for which Poisson's statistics were calculated. All data are plotted as the mean ± s.d.

50. Lévesque, J.-P. *et al.* Hematopoietic progenitor cell mobilization results in hypoxia with increased hypoxia-inducible transcription factor-1α and vascular endothelial growth factor A in bone marrow. *Stem Cells* **25**, 1954–1965 (2007).
51. Barbier, V., Winkler, I.G., Wadley, R. & Levesque, J.P. Flow cytometry measurement of bone marrow perfusion in the mouse and sorting of progenitors and stem cells according to position relative to blood flow *in vivo*. *Methods Mol. Biol.* **844**, 45–63 (2012).
52. Winkler, I.G. *et al.* Bone marrow macrophages maintain hematopoietic stem cell (HSC) niches and their depletion mobilizes HSC. *Blood* **116**, 4815–4828 (2010).
53. Barbier, V., Nowlan, B., Levesque, J.P. & Winkler, I.G. Flow cytometry analysis of cell cycling and proliferation in mouse hematopoietic stem and progenitor cells. *Methods Mol. Biol.* **844**, 31–43 (2012).
54. Barbier, V., Winkler, I.G. & Levesque, J.P. Mobilization of hematopoietic stem cells by depleting bone marrow macrophages. *Methods Mol. Biol.* **904**, 117–138 (2012).
55. Winkler, I.G., Hendy, J., Coughlin, P., Horvath, A. & Levesque, J.P. Serine protease inhibitors serpin1 and serpin3 are down-regulated in bone marrow during hematopoietic progenitor mobilization. *J. Exp. Med.* **201**, 1077–1088 (2005).
56. Shen, Y. *et al.* Tissue inhibitor of metalloproteinase-3 (TIMP-3) regulates hematopoiesis and bone formation *in vivo*. *PLoS ONE* **5**, e13086 (2010).